JJEE

Volume 11 | Number 4 | Pages 670-691

Jordan Journal of Electrical Engineering

ISSN (print): 2409-9600, ISSN (online): 2409-9619

Homepage: jjee.ttu.edu.jo

Variance-Omitted Sampling Technique (VoST) for Low Cost and High-Resolution AOA Estimation

Bakhtiar Ali Karim[1*]

[1] Department of Communication Engineering, Sulaimani Polytechnic University, Sulaimani 46001, Iraq
E-mail: bakhtiar.ali@spu.edu.iq

Received: Aug 11, 2025 *Revised: Oct 31, 2025* *Accepted: Nov 14, 2025* *Available online: Jan 20, 2026*

***Abstract*—** This manuscript introduces a robust and efficient sampling technique for optimizing data retrieval from large-dimension covariance matrix (CM). The proposed approach focuses on selecting the least-correlated and most-independent columns from the CM to construct the so-called projection matrix (PM) applied in angle of arrival (AOA) estimation. In contrast to the developed sampling techniques in literature, the recommended method excludes the signal variances located in the main diagonal of the CM during the column selection process. That is to say, the proposed technique focuses entirely on the off-diagonal elements of the CM that captures the covariance (correlations) between signals collected from different array elements. The proposed methodology is therefore named variance-omitted sampling technique (VoST). Applying this principle, we are able to extract the columns with minimal signal correlations corresponding to the off-diagonal entries of the CM and decrease the computational burden involved in the PM formulation process. To validate the theoretical claims and demonstrate the advantages of the proposed technique, a numerical example is provided, followed by extensive Monte Carlo simulations across several scenarios in which the performance of the proposed method is systematically compared with the existing techniques. The results demonstrate that VoST consistently surpasses previous algorithms in estimation resolution, root mean square error (RMSE), successful detection rate, ability to detect correlated signals, and computational speed.

***Keywords*—** AOA estimation; Covariance matrix sampling; Off-diagonal covariance matrix; Computational complexity; VoST.

1. INTRODUCTION

The estimation of signal parameters including frequency, polarization, and angle of arrival (AOA) has been an attractive research problem over a decade [1]. The AOA represents the direction from which transmitted signals reach the receiving antenna array. Accurate AOA estimation is crucial in many engineering applications, including radar [2, 3], patient monitoring [4], sonar [5], and wireless communications [6]. The performance of the newly developed smart antenna systems is merely determined by the accuracy of the AOA estimation techniques.

The outputs of these techniques are typically fed into an adaptive beamformer, which generates the main lobes and deep nulls as needed [7]. In MIMO systems, modeling space–time paths accurately are essential for ensuring reliable performance [8, 9]. Because the received data matrix in such systems is often large, employing an efficient sampling technique is practically important to enhance AOA estimation performance.

The broadly implemented AOA estimation algorithms in literature are minimum variance distortion less response (MVDR) [10], multiple signal classification (MUSIC) [11], minimum norm [12], and estimation of signal parameters via rotational invariant technique

* Corresponding author
DOI: https://doi.org/10.5455/jjee.204-1754938219

(ESPRIT)[13]. These algorithms require computationally demanding matrix operations such as matrix inversion, eigenvalue decomposition (EVD) or singular value decomposition (SVD) to identify the principal components of the large-size original matrix. Although these algorithms provide reliable estimation accuracy, they require intensive computational effort. This high complexity limits their suitability for real-time implementation.

Alternatively, linear AOA estimation algorithms such as propagator [14] and orthogonal propagator [15] are suggested to avoid such computational-hungry matrix operations through dividing the CM into small-dimension matrices. Although these algorithms guarantee considerable complexity reduction, they need to process all columns of CM which is unfeasible in case of massive MIMO systems.

To address the computation complexity issue, column-sampling techniques (CST) have emerged as an alternative solution [16]. CST extracts a limited number of columns from a high-dimensional matrix. The selected columns should closely represent the properties of the original matrix.

Mathematically, the sampled columns need to span almost the same subspace as the one obtained via EVD. From that perspective, several sampling techniques are proposed in literature including classical technique (CT) [17, 18], uniform technique (UT) [19], non-uniform technique (NUT) [20], and least correlated column sampling technique (LCCST) [21] to construct the so-called projection matrix (PM). CT extracts the first L-columns to construct the PM, where L represents the number of sources. However, its performance is limited because it relies only on static column selection, which cannot represent the overall characteristics of the original covariance matrix. UT is then proposed as an alternative approach for resolving the limitations of CT. UT enhances the AOA estimation performance via selecting the L-columns in a more distributed manner which increases the degree of freedom (DoF). Next, the NUT selects columns randomly from the CM. It aims to improve estimation performance by choosing L-columns with relatively higher energy. They show that applying the NUT increases the number of detectable sources significantly compared to the CT. Noticeably, the prevalent problem among the discussed techniques is that they ignore the correlation (i.e., dependency) between the selected columns, which limits the AOA estimation performance [22, 23].

Recently, a number of studies have addressed low-complexity AOA estimation from different perspectives. For example, Deng et al. in [24] propose a joint AOA/TOA UWB approach with reduced search dimensions; Shen et al. in [25] develop a root-SBL method for off-grid non-uniform arrays; Ahmad et al. [26] reduce dimensionality in 2D-DOD/DOA estimation; a compressive-sensing framework using coprime arrays appears in [27] ; and Yang et al. [28] explore coprime arrays with low-rank recovery under non-uniform noise. These works highlight the growing trend toward complexity-aware algorithm design, which underlines the relevance and novelty of the proposed VoST in this context.

To improve the estimation performance, an effective algorithm named LCCST is recently proposed. In this technique, the L-columns are chosen in an adaptive manner based on the correlation level within the CM columns. In other words, LCCST selects the columns with minimum dependency. This approach has been shown to significantly improve AOA estimation performance compared to existing techniques.

However, in LCCST a problem arises when attempting to compute the correlation within a given column. To be precise, the main diagonal of a covariance matrix (CM) represents the correlation of each signal with itself, also known as the signal variance. The off-diagonal

elements represent the correlations between signals received by different array elements, indicating how signals relate across the entire array. The focus here is on the correlation between different signals, that is, signals received from different array elements rather than the signal variance. Therefore, the off-diagonal elements of the CM should be used, and the main diagonal omitted during the column-norm calculation. Otherwise, we might end up with inaccurate correlation-level calculation and consequently selecting non-optimum samples for PM. This will result in degradation in the AOA estimation performance. To solve this fundamental problem in LCCST, we propose a new sampling methodology named variance-omitted sampling technique (VoST). The name stems from the fact that we omit the signal variance when we compute the column norm representing the correlation level between the signals of different elements. The sampled columns are then used to construct a PM named variance-omitted projection matrix (VoPM). The philosophy behind the suggested algorithm is that we exclude the correlation between signals themselves (i.e., signal variances) reside on the main diagonal of the CM during the column selection process. By doing so, we can focus and extract the columns which have minimum correlation between the collected signals. This adjustment to the recent LCCST ensures improved AOA estimation performance and reduced computational cost during the estimation process.

The key contributions of this paper can be concluded as follows:

- A new CM sampling technique named VoST has been proposed. In contrast to the existing algorithm, the proposed technique skips the signal variances sit on the main diagonal of the CM during the column section procedure. This refinement in column selection ensures the following benefits.
- VoST enables the extraction of optimal columns based on signal dependency, leading to improved resolution and accuracy in AOA estimation. That is to say, by excluding variances we remove the noise power terms from the CM, and this helps in improving the accuracy of the AOA estimation algorithm.
- VoST decreases the number of mathematical operations required for PM construction, resulting in reduced overall complexity of the algorithm.

The remaining parts of this paper are organized as follows. Section 2 presents the problem formulation for AOA estimation. In Section 3, the preceding sampling techniques for PM construction are revisited. Section 4 reveals the working principle of the proposed AOA estimation algorithm. The computational complexity of the existing and proposed techniques is analyzed in Section 5. In Section 6, the achieved simulation results are presented and comprehensively discussed. Section 7 concludes the key findings of the paper.

2. PROBLEM FORMULATION

To formulate the AOA estimation problem, we assume that a uniform linear array (ULA) with M elements is illuminated by L far-field sources as shown in Fig. 1. After receiving the signal by m-th element, it is down-converted to base-band signal which can be expressed by following equation:

$$x_m(t) = s_l(t - \Delta t_m)e^{-i2\pi f_c \Delta t_m} \quad (1)$$

where s_l is the emitted signal by l-th source. f_c denotes the carrier frequency and Δt_m is the propagation-delay of the signal received by m-th element with respect to reference (i.e., first) element.

$$\Delta t_m = \frac{d\ m\ sin\ \theta}{speed\ of\ light\ (c)} \quad (2)$$

when d is the spatial distance between two adjacent elements. θ denotes the AOA of the incident signal. Then, the down-converted signal is digitalized as follows:

$$x_m(nT) = s_l(nT - \Delta t_m)e^{-i2\pi f_c\,\Delta t_m} \quad (3)$$

where T represents the symbol period. In communication system ($T \gg \Delta t_m$), thus Eq. (3) can be approximately written as

$$x_m(nT) \approx s_l(nT)e^{-i2\pi f_c\,\Delta t_m} \quad (4)$$

As $d = ½\,\lambda$, and $c = f_c\,\lambda$, the above equation can be simplified as follows:

$$x_m(nT) \approx s(nT)e^{-i\,\pi\,k\ sin\,\theta} \quad (5)$$

For simplicity, we use discrete notation and Eq. (5) becomes

$$x_m[n] \approx s[n]e^{-i\,\pi\,k\ sin\,\theta} = s[n]a_m(\theta) \quad (6)$$

where $x_m[n]$ is the n-th sample of the signal at the m-th element which can be written as:

$$x_m[n] \approx \sum_{j=0}^{L-1} s_j[n]a(\theta_j) \quad (7)$$

where $s_j[n]$ represents the n-th symbol of the j-th signal, $j = 1,2,\ldots L-1$. Then, considering all the array elements, Eq. (7) can be expressed in a matrix form as follows:

$$\begin{bmatrix} x_0[n] \\ x_1[n] \\ . \\ . \\ . \\ x_{M-1}[n] \end{bmatrix} = \begin{bmatrix} a_0(\theta_0) & a_0(\theta_1) & . & . & . & a_0(\theta_{L-1}) \\ & & & . & & \\ & & & . & & \\ & & & . & & \\ a_{M-1}(\theta_0) & a_{M-1}(\theta_1) & . & . & . & a_{M-1}(\theta_{L-1}) \end{bmatrix} \begin{bmatrix} s_0(n) \\ s_1(n) \\ . \\ . \\ . \\ s_{L-1}(n) \end{bmatrix} + \begin{bmatrix} v_0\,(n) \\ v_1\,(n) \\ . \\ . \\ . \\ v_{M-1}\,(n) \end{bmatrix} \quad (8)$$

Here $v_m(n)$ is the statistically uncorrected additive white Gaussian noise at m-th element.

$$\boldsymbol{A} = [a\,(\theta_0)\ \ a\,(\theta_1)\ \ldots\ a\,(\theta_{L-1})] \quad (9)$$

where $\boldsymbol{A} \in \mathbb{C}^{M\,x\,L}$ is called steering matrix (i.e., array manifold), which contains the steering vectors $a\,(\theta_j)$ of source $s_j(n)$. Thus, Eq. (8) can be written in more compact form as follows:

$$\boldsymbol{x_n} = \boldsymbol{A}\,\boldsymbol{s_n} + \boldsymbol{v_n} \quad (10)$$

where $\boldsymbol{x_n} \in \mathbb{C}^{M\,x\,n}$ denotes the n-th received signal vector. $\boldsymbol{s_n}$ and $\boldsymbol{v_n}$ represent signal and noise vectors, respectively.

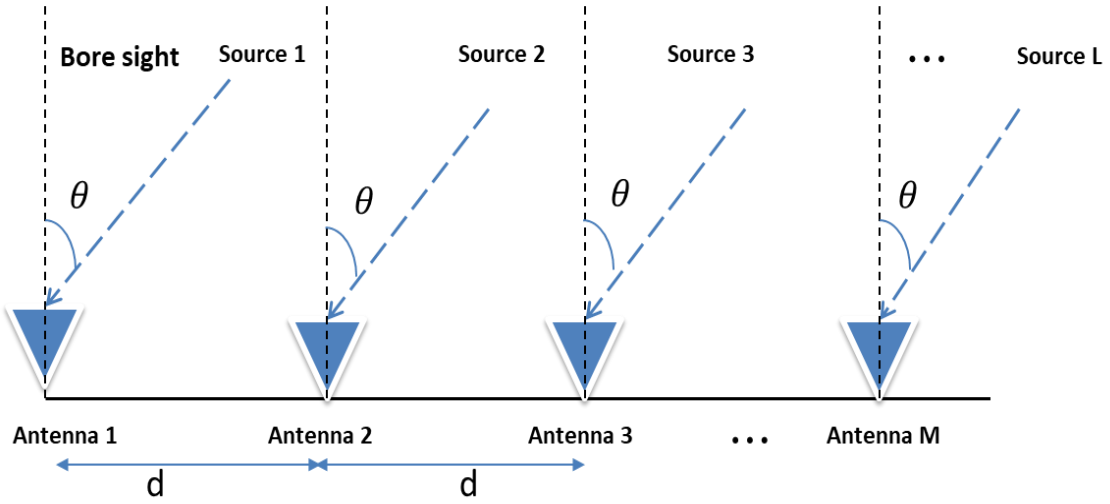

Fig. 1. AOA model considering M elements and L incident signals.

Although the array model in this work is presented using a ULA configuration for the sake of clarity and analytical simplicity, the proposed VoST is not restricted to this geometry. The algorithm operates directly on the covariance matrix of the received data, which can be constructed for any arbitrary array configuration (e.g., circular, planar, or 3D arrays). Therefore, the underlying principles and performance of VoST remain fully applicable to general array geometries.

3. EXISTING SAMPLING TECHNIQUES FOR PM CONSTRUCTION

To avoid the high computational cost involved with EVD, PM construction based on a limited number of columns (i.e., L-columns) of CM is widely adopted in AOA estimation. The estimation performance, however, is directly dependent on the accuracy of the column's selection, i.e., whether the selected columns span the intended subspace. In this section, we revisit the existing sampling techniques employed for PM construction and AOA estimation. To this end, we assume that N data samples have been collected by the ULA shown in Fig. 1 and the received data matrix is represented as follows:

$$\boldsymbol{X}(t) = \begin{pmatrix} x_1(t_1) & x_1(t_2) & \dots & \dots & x_1(t_N) \\ x_2(t_1) & x_2(t_2) & \vdots & \vdots & x_2(t_N) \\ \vdots & \vdots & \ddots & \vdots & \vdots \\ \vdots & \vdots & \vdots & \ddots & \vdots \\ x_M(t_1) & x_M(t_2) & \dots & \dots & x_M(t_N) \end{pmatrix} \tag{11}$$

$\boldsymbol{X}(t)$ is then used to compute the true CM $\boldsymbol{\mathcal{K}}_{xx}$ as follows:

$$\boldsymbol{\mathcal{K}}_{\mathbf{xx}} = \mathrm{E}[\mathbf{X}(\mathrm{t})\mathbf{X}(\mathrm{t})^{\mathrm{H}}] = \mathrm{E}[\mathbf{FS}(\mathrm{t})\mathbf{S}^{\mathrm{H}}(\mathrm{t})\mathbf{F}^{\mathrm{H}}] + \mathrm{E}[\mathbf{N}(\mathrm{t})\mathbf{N}^{\mathrm{H}}(\mathrm{t})]$$
$$\boldsymbol{\mathcal{K}}_{\mathrm{xx}} = \mathbf{F}\boldsymbol{\mathcal{K}}_{\mathrm{ss}}\mathbf{F}^{\mathrm{H}} + \sigma_{\mathrm{n}}^2\,\mathbf{I}_{\mathrm{M}} \tag{12}$$

where $\boldsymbol{\mathcal{K}}_{\mathrm{ss}} \in \mathbb{C}^{\mathrm{L}\times\mathrm{L}} = \mathrm{E}[\mathbf{s_n}\,\mathbf{s_n}^{\mathrm{H}}]$ is the desired signal CM. $\sigma^2\mathbf{I}_{\mathrm{M}}$ depicts the CM of noise where $\mathbf{I}_{\mathrm{M}}$ is an $M \times M$ identity matrix and σ^2 is the noise variance. $(.)^H$ and $E[.]$ denote Hermitian transpose and expectation operators, respectively. When the observed sources are non-stationary, the AOA value will fluctuate. Meaning that the content of $\boldsymbol{F}$ will change partially or completely, which implies that the content of the CM $\boldsymbol{\mathcal{K}}_{xx}$ will also change. Therefore, to track the signal properties of non-stationary sources and achieve an accurate estimation of AOA, the CM needs to be estimated periodically over N data samples as follows:

$$\boldsymbol{\mathcal{K}}_{xx} = \frac{1}{T}\sum_{t=1}^{T}\boldsymbol{X}(t)\boldsymbol{X}(t)^{\mathrm{H}} = \begin{bmatrix} \kappa_{11} & \kappa_{12} & \dots & \kappa_{1M} \\ \kappa_{21} & \kappa_{22} & \dots & \kappa_{2M} \\ \vdots & \vdots & \ddots & \vdots \\ \kappa_{M1} & \kappa_{M2} & \dots & \kappa_{MM} \end{bmatrix} \tag{13}$$

where T denotes the total number of data samples.

3.1. Classical Technique (CT)

The CT [17, 18] follows the simplest procedure to sample the L-columns from the CM for PM construction. This method simply extracts the information lying in the first L-columns and constructs the sampled matrix $\boldsymbol{S}$ as follows:

$$\boldsymbol{S}_{\mathrm{CT}} = \begin{bmatrix} \kappa_{11} & \kappa_{12} & \dots & \kappa_{1L} \\ \kappa_{21} & \kappa_{22} & \dots & \kappa_{2L} \\ \vdots & \vdots & \ddots & \vdots \\ \kappa_{M1} & \kappa_{M2} & \dots & \kappa_{ML} \end{bmatrix} \tag{14}$$

Based on Eq. (14), $\mathbf{S}_{\mathrm{CT}} = [\kappa_1\ \kappa_2\ \cdots\ \kappa_{\mathrm{L}}]$, where $\kappa_{1\le \mathrm{j}\le \mathrm{L}}$ represents the j-th column of original CM $\boldsymbol{\mathcal{K}}_{xx}$. Fig. 2 illustrates the concept of this column selection. In Fig. 2, the positions

of the (selected and unselected) columns are plotted again normalized column norm which is a representative of the correlation level between signals in that column.

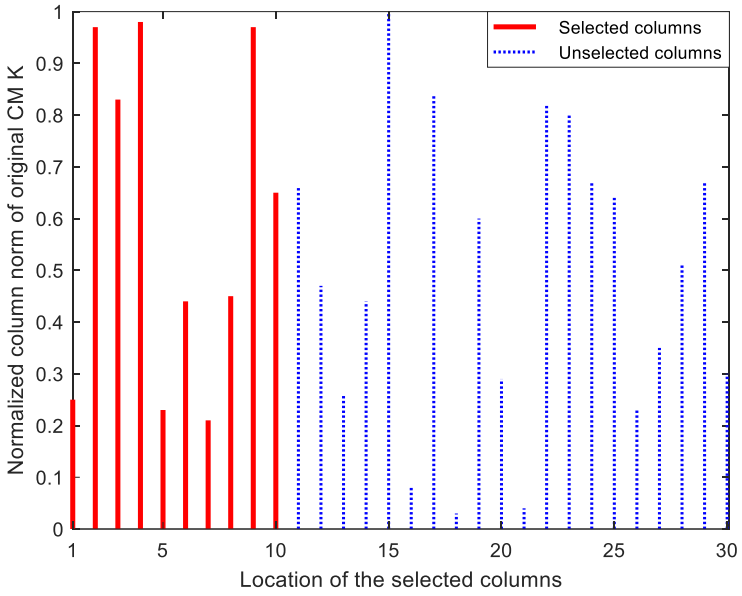

Fig. 2. Illustrative example of selecting ten columns ($\boldsymbol{L = 10}$) from $\boldsymbol{\mathcal{K}_{xx} \in \mathbb{C}^{30\times 30}}$ using CT.

Then, the CT constructs the PM as follows**:**

$$\mathbf{Q}_{\mathrm{CT}} = \mathbf{I}_{\mathrm{M}} - \mathbf{S}_{\mathrm{CT}} \left(\mathbf{S}_{\mathrm{CT}}^{\mathrm{H}} \mathbf{S}_{\mathrm{CT}}\right)^{-1} \mathbf{S}_{\mathrm{CT}}^{\mathrm{H}} \tag{15}$$

Then, the AOAs are estimated based on the peaks of the following function:

$$\mathbf{Y}_{\mathrm{CT}}(\theta, \phi) = \frac{\mathbf{1}}{\left\| \boldsymbol{f}^{H}(\theta,\phi)\mathbf{Q}_{\mathrm{CT}} \right\|^{\mathbf{2}}} \tag{16}$$

This CT's primary advantage lies in its simplicity. However, the algorithm has two essential problems. (i) the chosen columns are statics (predefined). It always relies on the information on the first L-columns and ignores others, resulting in low DoF. (ii) The selected columns may contain high correlation-level between signals (for example, see column 2 in Fig. 2). This makes the columns of the sampled matrix $\mathbf{S}_{\mathrm{CT}}$ to be highly dependent. Hence, $\mathbf{S}_{\mathrm{CT}}$ will not be a good representative of the general trends of the CM. These two fundamental issues will limit the performance of the CT, hence the corresponding AOA estimation algorithm.

3.2. Uniform Technique (UT)

In comparison to the CT, UT [19] aims to improve the DoF by selecting the same number of columns. To this end, the UT adopts a more distributed approach (rather than simply selecting the first L-columns) to identify a better position of the columns to be chosen for PM construction. Therefore, the sampled matrix of UT, $\mathbf{S}_{\mathrm{UT}}$**,** is formed based on the following formula.

$$\mathbf{S}_{\mathrm{UT}} = \left\{ \mathrm{c_i} | \mathrm{c_i} = 1 + \mathrm{round}\left(\frac{(\mathrm{i}-1)(\mathrm{M}-1)}{\mathrm{L}-1} \right)_{\mathbf{i}=\{1,2\ldots,\mathrm{L}\}} \right\} \tag{17}$$

where c_i represents the indices of the selected columns for $1 \leq i \leq L$. The conceptual diagram of column selection based on the UT is illustrated in Fig. 3. The advantage of the UT is its ability to enhance the DoF by selecting columns in a more distributed manner. However, this uniform column-selection is still not adaptive. Additionally, the UT selects columns with high column norm (high correlation between signals) for example, see column 4 in Fig. 3. Then, the

UT follows the same procedure as CT through applying Eq. (15), with replacing $\mathbf{S}_{\mathrm{CT}}$ to $\mathbf{S}_{\mathrm{UT}}$, and Eq. (16) to estimate the location of the sources.

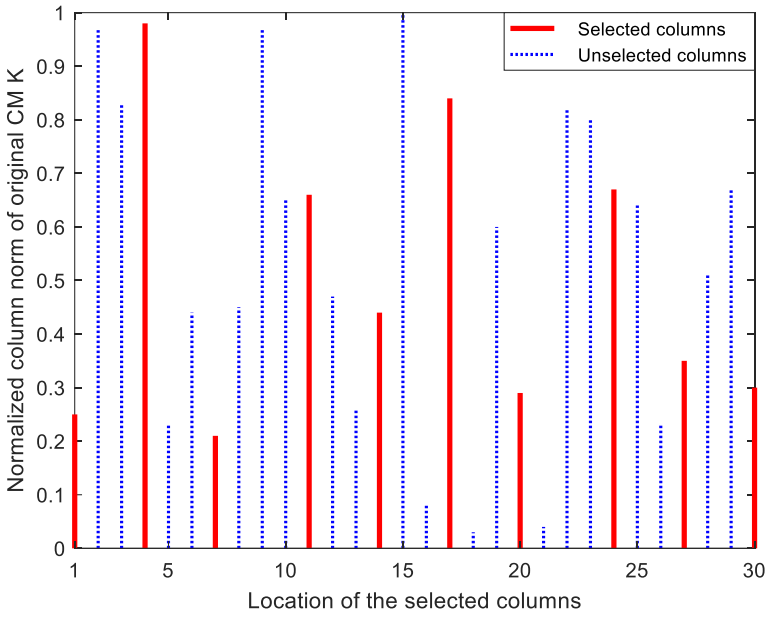

Fig. 3. Illustrative example of selecting ten columns ($L = 10$) from $\boldsymbol{\mathcal{K}}_{xx} \in \mathbb{C}^{30\times30}$ using UT.

3.3. Non-uniform Technique (NUT)

NUT suggested in [20] is another attempt made to improve the estimation performance of the CT through increasing the signal eigenvalues' energy. Unlike the CT and UT, NUT selects the columns in a non-predefined fashion by randomly choosing L-columns from $\boldsymbol{\mathcal{K}}_{xx}$ to construct the sampled matrix $\mathbf{S}_{\mathrm{NUT}}$ as illustrated in Fig. 4.

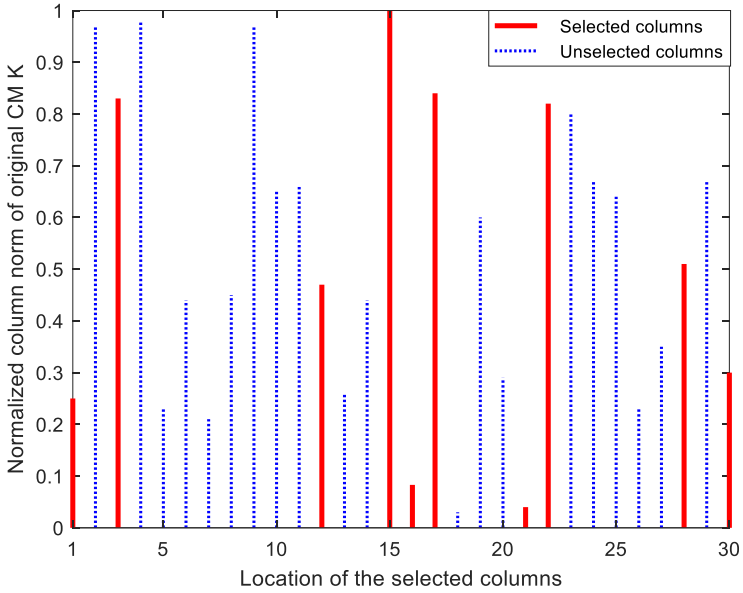

Fig. 4. Illustrative example of selecting ten columns ($L = 10$) from $\boldsymbol{\mathcal{K}}_{xx} \in \mathbb{C}^{30\times30}$ using NUT.

The NUT performs column selection in a non-static, random manner. However, it still fails to address the problem of selecting columns with high correlation, indicated by large column norms.

After constructing the sampled matrix $\mathbf{S}_{\mathrm{NUT}}$, the NUT adheres to the same process as CT through applying Eq. (15), with replacing $\mathbf{S}_{\mathrm{CT}}$ to $\mathbf{S}_{\mathrm{NUT}}$, and Eq. (16) to generate the spatial spectrum.

3.4. Least Correlated Column Sampling Technique (LCCST)

LCCST is the latest attempt made to improve the AOA estimation performance through selecting optimum positions of the columns. As discussed above, a key limitation shared by all previous methods is the selection of columns with high correlation, where a large column norm indicates strong signal dependency.

To address this issue, LCCST is proposed in [21]. In this technique, the column norm is used a measure of correlation level between signals collected from different array elements (i.e., higher norm means higher correlation and vice versa). Therefore, the sampled matrix based on the LCCST $\mathbf{S}_{\mathrm{LCCST}}$ is formed as follows:

$$\mathbf{S}_{\mathrm{LCCST}} = \left[\begin{Bmatrix} \kappa_{11} \\ \kappa_{21} \\ \vdots \\ \kappa_{\mathrm{M1}} \end{Bmatrix} \begin{Bmatrix} \kappa_{1c} & \cdots & \kappa_{1c} \\ \kappa_{2c} & \cdots & \kappa_{2c} \\ \vdots & \ddots & \vdots \\ \kappa_{\mathrm{Mc}} & \cdots & \kappa_{\mathrm{Mc}} \end{Bmatrix} \begin{Bmatrix} \kappa_{1\mathrm{M}} \\ \kappa_{2\mathrm{M}} \\ \vdots \\ \kappa_{\mathrm{MM}} \end{Bmatrix} \right] \tag{18}$$

Here, c represents the set of column numbers defined as:

$$c = \{\mathcal{E} |\ \mathcal{E} = \{2,3 \ldots, M-1\}\} \tag{19}$$

where $\mathcal{E}$ is a set of integer numbers. This algorithm selects the $L-2$ columns (provided that first and last columns are already selected as shown in Eq. (15) based on the following formula:

$$c_s = Position\ ([mink\ (\{\|\kappa_c\|_2\}, L-2)]\ ),$$

$$c_u = Position\ ([maxk\ (\{\|\kappa_c\|_2\}, M-L)]\ ),$$

where *mink* and *maxk* are the two functions that return *L-2* minimums and $M-L$ maximums from their arguments ($\{\|\kappa_c\|_2\}$). $||.||$ is the norm operator which returns the column norm and it *includes* the signal variance (main diagonal of the CM) into its calculation. The column selection based on the LCCST is illustrated in Fig. 5, where the selected columns show low correlation (represented in a normalized norm form) compared to the unselected ones.

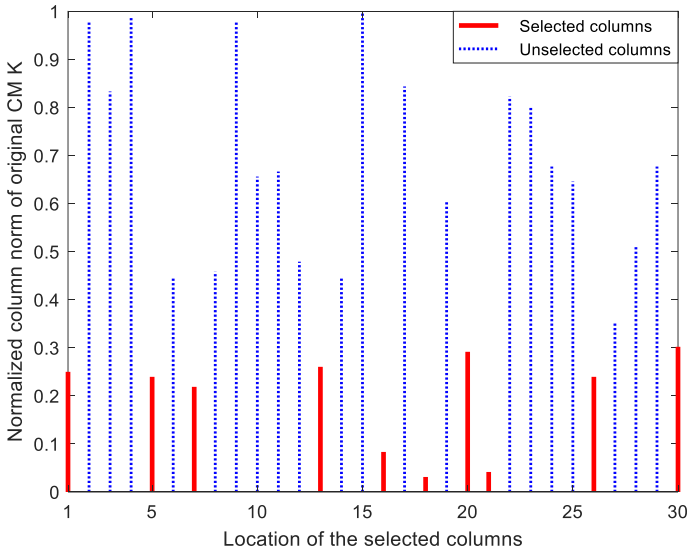

Fig. 5. Illustrative example of selecting ten columns ($L = 10$) from $\mathcal{K}_{\mathrm{xx}} \in \mathbb{C}^{30\times30}$ using LCCST.

Then, the LCCST follows the same procedure as the abovementioned techniques, using $\mathbf{S}_{\mathrm{LCCST}}$ to form the PM then applies it in the spatial construction Eq. in (16).

While the LCCST attempts to choose columns with minimal correlation, the process of calculating the column norm needs to be refined. The main diagonal of the CM represents the signal variances, often referred to as noise power, while the off-diagonal elements describe the covariance—or correlation—between signals received by different array elements. For precise correlation level determination between signals, the main diagonal elements of the CM should be omitted when computing column norms. This issue is addressed by introducing a new technique which offers several advantages as presented in the following section.

4. PROPOSED AOA ESTIMATION ALGORITHM

The problem with the recently developed LCCST is that it incorporates the signal variances into the calculation of the column norm of the observed CM. This may mislead the estimator as the correlation between the signals does not rely on the signal variance; it purely relies on the signal covariance (located on the off-diagonal of CM). To address this problem, we propose a new sampling technique in this section.

4.1. Variance-omitted Sampling Technique (VoST)

Similar to the previous work in [21], we sample L-columns from M ($L < M$) based on the correlation between the signals across the antenna array. In contrast to [21], which incorporates the signal variances located on the main diagonal of the CM into the column-norm calculation, we exclude them by setting the signal variances to zero as shown in Eq. (20). The principle of our technique stems from the fact that the variances (i.e., diagonal elements of the CM) represent the individual noise power at each antenna element. These terms may not contribute significantly to angle estimation since we are more interested in how signals relate to each other across the array. This variance omission thus allows for a more accurate calculation of the correlation (expressed in covariance form) between signals collected from different array elements. Therefore, before calculating the correlation between signals using the column norms, we apply a preprocessor to remove the variances from the original CM and generating off-diagonal CM (ODCM) as follows:

$$\widehat{\boldsymbol{\mathcal{K}}}_{xx} = \boldsymbol{\mathcal{K}}_{\mathrm{xx}} - \mathrm{diag}(\boldsymbol{\mathcal{K}}_{\mathrm{xx}}) = \begin{bmatrix} \mathbf{0} & \kappa_{12} & \kappa_{13} & \dots & \kappa_{1M} \\ \kappa_{21} & \mathbf{0} & \kappa_{23} & \cdots & \kappa_{2M} \\ \kappa_{31} & \kappa_{32} & \mathbf{0} & \dots & \kappa_{3M} \\ \vdots & \vdots & \vdots & & \vdots \\ \kappa_{M1} & \kappa_{M2} & \cdots & \kappa_{MM-1} & \mathbf{0} \end{bmatrix} \tag{20}$$

where $\widehat{\boldsymbol{\mathcal{K}}}_{xx}$ represents the ODCM and κ_{12} denotes the covariance (relationship) between signal received from array element 1 and element 2, and $\mathrm{diag}(\boldsymbol{\mathcal{K}}_{\mathrm{xx}}) = \mathrm{diag}(\kappa_{11},\ \kappa_{22}, \dots, \kappa_{MM})$ After that, we compute the norm for each column of $\widehat{\boldsymbol{\mathcal{K}}}_{xx}$ where each column represents the actual correlation between signals collected from different array elements. We subsequently select the columns with the relatively smallest norm values, indicating that these columns contain the least correlation between signals. The sampled matrix obtained from the ODCM is as follows:

$$\mathbf{S}_{\mathrm{VoST}} \in \mathbb{C}^{\mathrm{M\times L}} = \begin{Bmatrix} \mathbf{0} & \kappa_{1c} & \kappa_{1c} \\ \kappa_{2c} & \mathbf{0} & \kappa_{2c} \\ \kappa_{\mathrm{Mc}} & \kappa_{\mathrm{Mc}} & \mathbf{0} \end{Bmatrix} \tag{21}$$

where $c = c_i | c_i$ is a unique variable representing the column indices and defined as follows:

$$c_i = \{\mathbb{Z}_M = \{1,2,\dots,M\} \text{ for } i = \{1,2,\dots L\}\} \tag{22}$$

To be precise, c denotes the indices (i.e., positions) of L selected columns (c_s) and $M-L$ unselected columns (c_u). The fundamental problem here is how we can extract L-columns from M ($L < M$) that span almost the same spaces as the original signals subspace obtain by EVD. We address this problem by selecting the columns based on their *pure* norms (excluding the signals' variances reside on the main diagonal of the CM during the column norm calculation). Mathematically, the proposed technique selects L -columns based on the following equation:

$$c = \begin{cases} c_s\ , & \nmid \kappa_{c_s} \nmid = min\left\{\nmid \kappa_{c_s} \nmid\right\} \quad for\ 1 \le s \le L \\ c_u\ , & \nmid \kappa_{c_u} \nmid = max\left\{\nmid \kappa_{c_u} \nmid\right\} \quad for\ 1 \le u \le M-L \end{cases} \tag{23}$$

where $\nmid . \nmid$ denotes the operator which calculates the column-norm ***excluding*** the main diagonal elements, *max* and *min* are the functions that return the maximum and minimum values from $\nmid \kappa_c \nmid$ for a given value of u and s, respectively. Relying on Eq. (23), the selected columns exhibit minimum correlation between the signals in comparison to the unselected columns, and this consequently makes the selected columns to be *least dependent* as it is proven in [21]. This feature of the proposed technique is particularly important because it ensures the extraction of columns with completely non-redundant information about the signals arriving at the receiving array. That is to say, the components of each source are uniquely represented by a single column of the sampled matrix $\mathbf{S}_{\mathrm{VoST}}$. The suggested methodology thus guarantees higher estimation performance in comparison to not only CT, UT, NUT, but also the newly developed LCCST as will be shown in the following sections.

We here do not rely on the norm calculations from the previous sections (e.g., in Fig. 5), as they include the signal variance by calculating the column norm from the original CM $\boldsymbol{\mathcal{K}}_{xx}$. So, we compute a new column-norm for the ODCM $\widehat{\boldsymbol{\mathcal{K}}}_{xx}$ and then select the L-columns based on minimum norm values which reflect the *actual* correlation between signals. The conceptual illustration of the proposed technique is shown in Fig. 6.

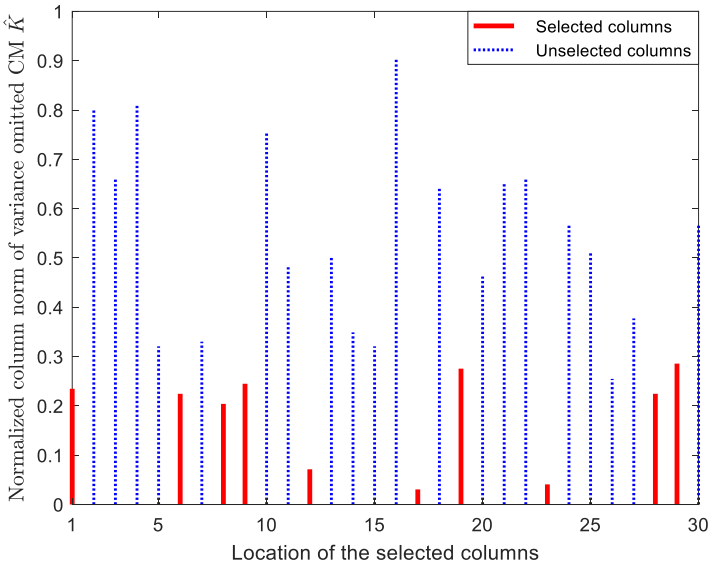

Fig. 6. Illustrative example of selecting ten columns ($L = 10$) from $\mathcal{K}_{\mathrm{xx}} \in \mathbb{C}^{30\times30}$ using proposed VoST.

Compared to Fig. 5, the overall column norm in Fig. 6 is reduced due to the exclusion of the signal variance in the norm calculation. Importantly, in Fig. 6, the columns are selected based on minimum norms which realistically represent the true signal-correlations. It is

proven in [21] that selecting columns with minimum norm results in lower dependency between selected columns (i.e., each column contains non-redundant information about the signal sources). This leads to higher estimation performance of the proposed algorithm. Table 1 shows and compares the strengths and weaknesses of different sampling techniques applied to AOA estimation.

Table 1. Advantages and limitations of various CM sampling techniques.

Algorithm	Advantage	Limitations
CT [17, 18]	(i)Simplicity.	(i)Positions of the selected columns are predefined. (ii) Limited DoF. (iii) High correlation between selected columns.
UT [19]	(i)Enhancing DoF.	(i) The columns are selected in a static fashion. (ii) High correlation between selected columns.
NUT [20]	(i)Increasing signal eigenvalues.	(i)High correlation between selected columns.
LCCST [21]	(i)Minimizing correlation between selected columns.	(i) Incorporating the signal variance into the column norm calculation (i.e., inaccurate correlation-level calculation).
Proposed	(i) Optimizes the column-norm calculation to overcome the LCCST limitations. (ii)Achieves more accurate correlation-level estimation. (iii) Guarantees higher AOA estimation accuracy with lower computational complexity.	(i) No significant drawbacks observed in the current evaluation.

While omitting the main diagonal of the CM enhances the accuracy of inter-signal correlation estimation, it may slightly reduce the total signal energy captured by the model under very low-SNR conditions.

Nevertheless, in such scenarios, the off-diagonal elements remain the principal contributors to accurate AOA estimation, as they characterize the true spatial dependencies between array elements. Moreover, as shown in Section 6.2, the proposed VoST retains robust estimation accuracy even at low SNR values, validating that the omission of the diagonal does not compromise overall performance.

4.2. PM and AOA Estimation based on VoST

The VoPM is formulated based on the proposed VoST as follows:

$$\mathbf{Q}_{\mathrm{VoST}} = \mathbf{I}_{\mathrm{M}} - \mathbf{S}_{\mathrm{VoST}}\left(\mathbf{S}_{\mathrm{VoST}}^{\mathrm{H}}\,\mathbf{S}_{\mathrm{VoST}}\right)^{-1}\,\mathbf{S}_{\mathrm{VoST}}^{\mathrm{H}} \tag{24}$$

The angle of the incident signals is calculated based on the proposed algorithm using the following formula:

$$\boldsymbol{Y}_{\mathrm{VoST}}(\theta,\phi) = \frac{\mathbf{1}}{\left\|\boldsymbol{f}^{H}(\theta,\phi)\mathbf{Q}_{VoST}\right\|^{\mathbf{2}}} \tag{25}$$

The main steps of the proposed AOA estimation are summarized as below.

Algorithm 1: Variance-omitted sampling technique VoST for accurate AOA estimation.

Requires	**The received data $\boldsymbol{X} \in \mathbb{C}^{M \times N}$ with $\boldsymbol{M}$ array elements, $\boldsymbol{N}$ data samples, and $\boldsymbol{L}$ sources.**
Ensures	**Cost efficient and accurate AOA estimation.**
Step 1	Compute the received signal and add Gaussian noise with a certain SNR.
Step 2	Calculate the CM $\boldsymbol{\mathcal{K}}_{xx}$ for the received signal using Eq. (13)
Step 3	Set the main diagonal of $\boldsymbol{\mathcal{K}}_{xx}$ to zero to generate $\widehat{\boldsymbol{\mathcal{K}}}_{xx}$ (transforming CM to ODCM)
Step 4	Compute the norm for each column of ODCM $\widehat{\boldsymbol{\mathcal{K}}}_{xx}$
Step 5	Sort the results of **Step 4** in ascending order and determine their corresponding column positions (indices).
Step 6	Save the L-leading indices in an indexing set $\mathbf{i}$.
Step 7	Sort the indices values in $\mathbf{i}$ in ascending order.
Step 8	Select L-columns from $\widehat{\boldsymbol{\mathcal{K}}}_{xx}$ as $\boldsymbol{S}_{VoST} = \widehat{\boldsymbol{\mathcal{K}}}_{xx}(:, \mathbf{i})$.
Step 9	Compute the VoPM $\mathbf{Q}_{\mathrm{VoST}}$ using Eq. (24).
Step 10	Estimate AOA using Eq. (25).

5. THEORETICAL ANALYSIS OF COMPUTATIONAL COMPLEXITY

Formulating PM based on the traditionally-used sampling algorithms applied to an $M \times L$ matrix $\mathbf{S}_x$[1] requires a computational cost of $\boldsymbol{O(M^2 L)}$. This is because the resulting matrix is $M \times M$ and we need to compute the dot product between a row of $\mathbf{S}_x$ and a column of $\boldsymbol{S}_x^H$ where each needs L multiplications.

In the proposed technique, we bypass computations involving the zero elements located on the main diagonal of the CM (i.e., signal variances). That is to say, we generate the PM based on ODCM rather than the original CM. Thus, the overall computational cost of PM based on the proposed algorithm (see Eq. (24)) can be analyzed as follows:

1. Computation of $\mathbf{S}_{\mathrm{VoST}}^{\mathrm{H}} \mathbf{S}_{\mathrm{VoST}}$
   - $\mathbf{S}_{\mathrm{VoST}}^{\mathrm{H}}$ is an $L \times M$ and $\mathbf{S}_{\mathrm{VoST}}$ is $M \times L$, so the result is an $L \times L$ matrix.
   - The standard cost that is usually paid for this multiplication is $\boldsymbol{Cost_{Traditional} = O(L^2 M)}$.
   - As $\mathbf{S}_{\mathrm{VoST}}$ has zero-elements on its diagonal (i.e., signals variances are omitted in the computation), each dot product between a row of $\mathbf{S}_{\mathrm{VoST}}^{\mathrm{H}}$ and a column of $\mathbf{S}_{\mathrm{VoST}}$ involves $M - 1$ terms rather than M.
   - The cost based on the proposed algorithm for $\mathbf{S}_{\mathrm{VoST}}^{\mathrm{H}} \mathbf{S}_{\mathrm{VoST}}$ becomes $\boldsymbol{Cost_{New} = O(L^2(M-1))}$.

[1] $\boldsymbol{S}_x$ is a representative of $\boldsymbol{S}_{\mathrm{CT}}, \boldsymbol{S}_{\mathrm{UT}}, \boldsymbol{S}_{\mathrm{NUT}}$, and $\boldsymbol{S}_{\mathrm{LCCST}}$.

2. Computation of $(\mathbf{S}_{\mathrm{VoST}}^{\mathrm{H}}\,\mathbf{S}_{\mathrm{VoST}})^{-1}$
   - Generally, the inverse of an $L \times L$ matrix needs $O(L^3)$ operations using methods like LU decomposition or Gaussian elimination.
   - We cannot guarantee the direct complexity reduction due to the zeros in $\mathbf{S}_{\mathrm{VoST}}$ because the inverse operation on $\mathbf{S}_{\mathrm{VoST}}^{\mathrm{H}}\,\mathbf{S}_{\mathrm{VoST}}$, which is already an $L \times L$ matrix with non-zero entries. This step requires the following cost: $\boldsymbol{Cost_{New}} = \boldsymbol{Cost_{Traditional}} = \boldsymbol{O(L^3)}$
3. Computation of $\mathbf{S}_{\mathrm{VoST}}(\mathbf{S}_{\mathrm{VoST}}^{\mathrm{H}}\,\mathbf{S}_{\mathrm{VoST}})^{-1}$
   - This involves the multiplications between $M \times L$ $\mathbf{S}_{\mathrm{VoST}}$ with the $L \times L$ $(\mathbf{S}_{\mathrm{VoST}}^{\mathrm{H}}\,\mathbf{S}_{\mathrm{VoST}})^{-1}$.
   - The standard cost therefore is $\boldsymbol{Cost_{Traditional}} = \boldsymbol{O(ML^2)}$.
   - Since $\mathbf{S}_{\mathrm{VoST}}$ has zero-diagonal elements, the cost based on the proposed algorithm is reduced to $\boldsymbol{Cost_{New}} = \boldsymbol{O(M \times L \times (L-1))}$.
4. Computation of the final matrix $\mathbf{S}_{\mathrm{VoST}}(\boldsymbol{S}_{VoST}^{H}\,\mathbf{S}_{\mathrm{VoST}})^{-1}\boldsymbol{S}_{VoST}^{H}$
   - This step involves the multiplication between $\mathbf{S}_{\mathrm{VoST}}(\mathbf{S}_{\mathrm{VoST}}^{\mathrm{H}}\,\mathbf{S}_{\mathrm{VoST}})^{-1}$ which is $M \times L$, and the $\mathbf{S}_{\mathrm{VoST}}^{\mathrm{H}}$,which is $L \times M$. The standard cost is $\boldsymbol{Cost_{Traditional}} = O(M^2L)$.
   - Due to the zero-elements on the diagonal, each dot product between a row of $\mathbf{S}_{\mathrm{VoST}}$ and a column of $\mathbf{S}_{\mathrm{VoST}}^{\mathrm{H}}$ involves $L-1$ non-zero terms. The adjusted cost based on the proposed algorithm becomes $\boldsymbol{Cost_{New}} = \boldsymbol{O(M^2\,(L-1))}$.

   The total cost of formulating PM based on the proposed method is

   $$\boldsymbol{O\left(L^2(M-1)\right) + O\left(L^3\right) + O\left(M \times L \times (L-1)\right) + O\left(M^2 \times (L-1)\right)}$$

   For $M > L$, the overall cost therefore becomes

   $$\boldsymbol{Cost_{Overall\ New} = O\left(M^2 \times (L-1)\right)}$$

Which represents a notable reduction in computational complexity compared to traditional approaches that require full-matrix operations. The overall cost of PM construction applied in the previous works and that applied in this work are listed in Table 2.

Table 2. Computational cost of PM construction based on different sampling techniques.

PM construction steps	Complexity using CT, UT, NUT, LCCST	PM construction steps	Complexity using VoST
$\mathbf{S}_x^H\mathbf{S}_x$	$O(L^2M)$	$\mathbf{S}_{\mathrm{VoST}}^{\mathrm{H}}\,\mathbf{S}_{\mathrm{VoST}}$	$O\left(L^2(M-1)\right)$
$(\mathbf{S}_x^H\mathbf{S}_x)^{-1}$	$O(L^3)$	$(\mathbf{S}_{\mathrm{VoST}}^{\mathrm{H}}\,\mathbf{S}_{\mathrm{VoST}})^{-1}$	$O(L^3)$
$\mathbf{S}_x(\mathbf{S}_x^H\mathbf{S}_x)^{-1}$	$O(ML^2)$	$\mathbf{S}_{\mathrm{VoST}}(\mathbf{S}_{\mathrm{VoST}}^{\mathrm{H}}\,\mathbf{S}_{\mathrm{VoST}})^{-1}$	$O(M \times L \times (L-1))$
$\mathbf{S}_x(\mathbf{S}_x^H\mathbf{S}_x)^{-1}\mathbf{S}_x^H$	$O(M^2L)$	$\mathbf{S}_{\mathrm{VoST}}(\mathbf{S}_{\mathrm{VoST}}^{\mathrm{H}}\mathbf{S}_{\mathrm{VoST}})^{-1}\mathbf{S}_{\mathrm{VoST}}^{\mathrm{H}}$	$O\left(M^2\,(L-1)\right)$
Overall cost	$\boldsymbol{O(M^2L)}$	**Overall cost**	$\boldsymbol{O\left(M^2\,(L-1)\right)}$

6. RESULTS AND DISCUSSIONS

In this section, we compare the performance of the proposed algorithm to its counterparts by conducting multiple computer simulations over a wide range of scenarios. In the performance comparison, we apply average root mean square error (ARMSE) and probability of successful detection (P_d) as performance indicator and calculated as follows:

$$\mathrm{ARMSE} = \frac{1}{A}\sum_{i=1}^{a}\sqrt{\frac{1}{L}\sum_{j=1}^{L}\left[\left(\theta_j - \hat{\theta}_j\right)^2\right]} \tag{26}$$

$$\mathrm{P}_d(\mathrm{AOA}) = \frac{\sum_{i=1}^{A} \mathcal{D}_i}{AL} \quad (27)$$

Here A denotes the total number of Monte Carlo trials. θ_j and $\hat{\theta}_j$ represent the original and estimated AOAs at the jth trial, respectively. $\mathcal{D}_i$ is the total number of successful detections at ith trials.

6.1. Resolution Capability

When the signal sources are closely located, miss-detection becomes the essential problem for AOA estimators. From that perspective, we compare the resolution[2] capability of the proposed algorithm to its counterparts using the simulation parameters listed in Table 3. To make a fair comparison, we apply a severe test in which three-sets of three closely located sources transmit their signals toward the receiving array. Then, the procedures of the algorithms under the test are adopted to resolve the locations of these sources. The results achieved are shown in Fig. 7.

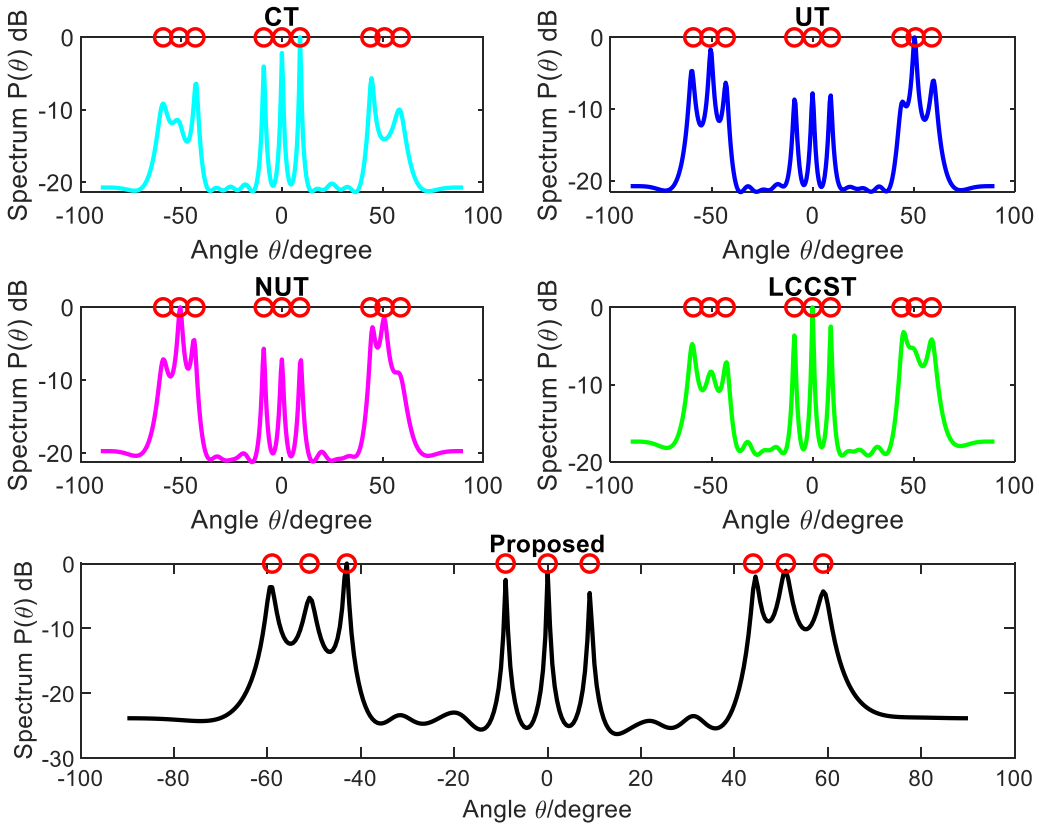

Fig. 7. The resolution performance of the VoST method is compared with CT, UT, NUT, and LCCST for nine AOAs, where the three-sets of three closely spaced AOAs present a severe test.

As illustrated, the compared algorithms show low resolution as they were not abe to identify the spatial locations of all the sources. In other words, they all sufer from a situaltion in which the three-sources are detected as two-sources experiencing at least one false-detection. On the other hand, the proposed algorithm accurately and unambiguously resolved the directions of all incoming signals by producing nine distinct peaks corresponding to the

[2] Resolution is defined as the ability of the AOA estimator to detect the closely located sources.

locations of their sources without any missed detections. The suggeted AOA estimator thus demonstrates higher resoution capability, which ends up with detecting comparatively higher number sources. Moreover, the noise immunity achieved through the proposed sampling technique is superior compared to previous technqiues. It is improtant to note that this high resoutluion capabilty of the proposed algorithm is due to the newly-adapted sampling methodolgy (i.e., VoST) to contsrut the PM.

Table 3. Simulation parameter for this scenario.

Parameter	Value
M	30
L	9
N	100
SNR	0 dB
Actual AOAs	-59° -51° -43° -9° 0° 9° 44° 51° 59°

6.2. Accuracy Comparison based on Varying SNR

This section aims to evaluate the impact of changing the SNR levels on the estimation accuracy[3] of the proposed method and other sampling techniques. To achieve this, we compute the ARMSE and P_d of the proposed algorithm and compare those with that for CT, UT, NUT, and LCCST based on different SNRs. This simulation is configured using the parameters listed in Table 4. One thousand Monte Carlo simulations (A = 1000) are conducted to generate ten random AOAs within the angular range of $-90°, 90°$. These angles are applied consistently across all the techniques to ensure a fair comparison. Then, the ARMSE and corresponding successful detections are calculated at each SNR level. The results obtained are plotted in Fig. 8 and Fig. 9, respectively. From the figures, it is evident that CT offers the least accuracy among the competing methods, followed by the UT, NUT, and LCCST, respectively. As shown, due to the minimal dependency between the selected columns obtained through applying the VoST, the proposed AOA estimation algorithm shows superior estimation accuracy achieving minimum ARMSE and highest successful detections across the entire SNR ranges compared to its counterparts.

Table 4. Simulation parameters for this scenario.

Parameters	Value
M	30
L	10
N	100
AOA	Random between $-90°$ and $90°$
SNR	Variying between -10 dB and 5 dB.
Monte Carlo trials, A	1000

6.3. Accuracy Comparison Based on the Correlation between Incoming Signals

Spatial smoothing technique is usually applied as a pre-processor to remove the negative impact of correlation among the signals on the AOA estimation technique. This solution, however, incurs the drawback of increased computational burden. To ensure low computational complexity, it is essential for the signal processing technique (e.g., AOA

[3] Estimation accuracy here is determined by the values of ARMSE and probability of successful detection P_d.

estimator) to effectively manage correlated sources in an intelligent manner. Therefore, this scenario examines how correlations between signals impact the performance of the AOA techniques considered. To achieve this, we assume that the incident signals are correlated due to multipath effects and ten correlated signals (L = 10) striking the same array as in the earlier scenarios. Precisely, we assume that there is just one signal source and the other incident signals are the result of reflections from this primary source. To model this scenario, we change the correlation level between the first signal and the subsequent ones as $r = [0.1\ 0.2\ 0.4\ 0.6\ 0.8]$. Other simulation parameters are listed in Table 5. For each value of r, we compute the accuracy criteria (i.e., ARMSE and P_d) over several trials and the average values are plotted as shown in Fig. 10 and Fig. 11.

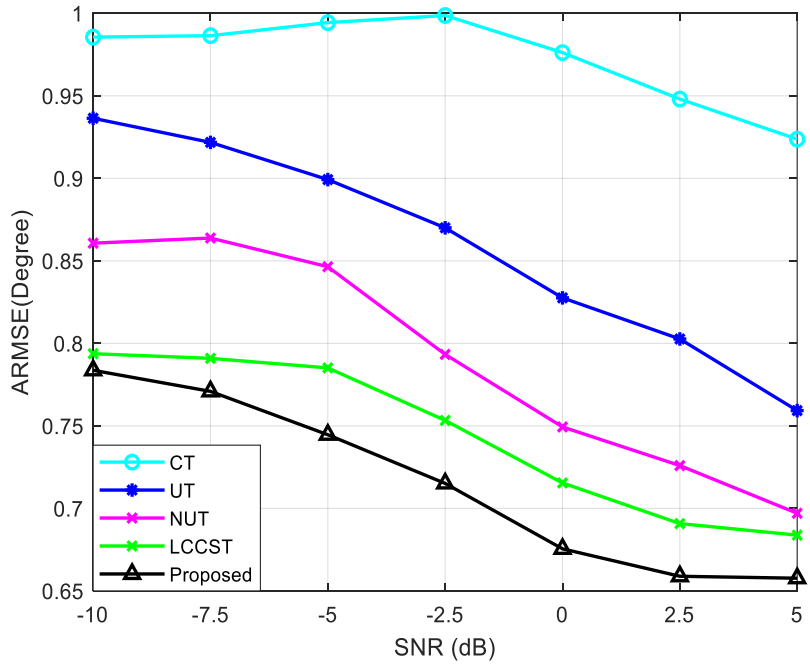

Fig. 8. Comparison of accuracy (ARMSE) between VoST and existing sampling techniques based on SNR variation.

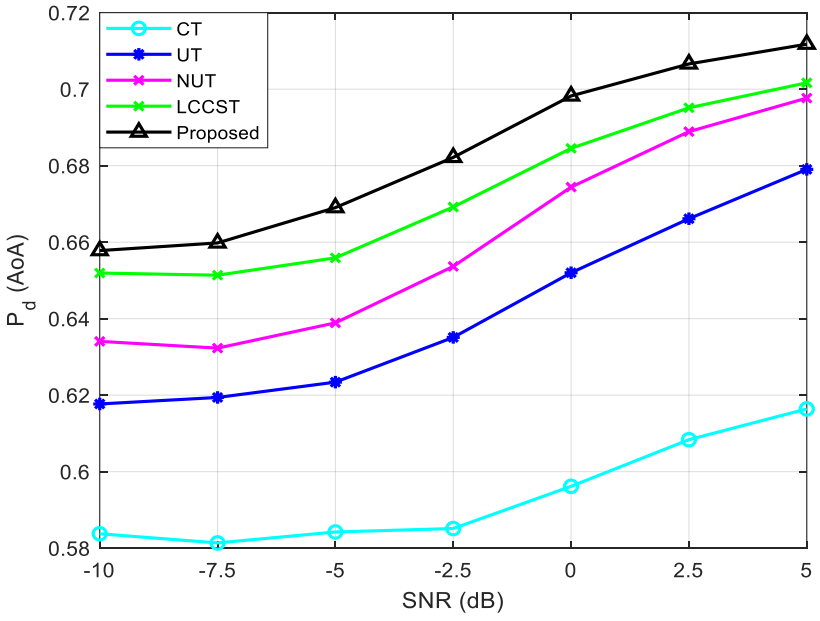

Fig. 9. Comparison of accuracy (P_d) between the VoST and existing sampling techniques based on SNR variation.

Table 5. Simulation parameters for this scenario.

Parameters	Value
M	30
L	10
N	100
AOA	Random between −90° and 90°
SNR	5 dB
Monte Carlo trials, A	5000
Correlation between signals	Vary

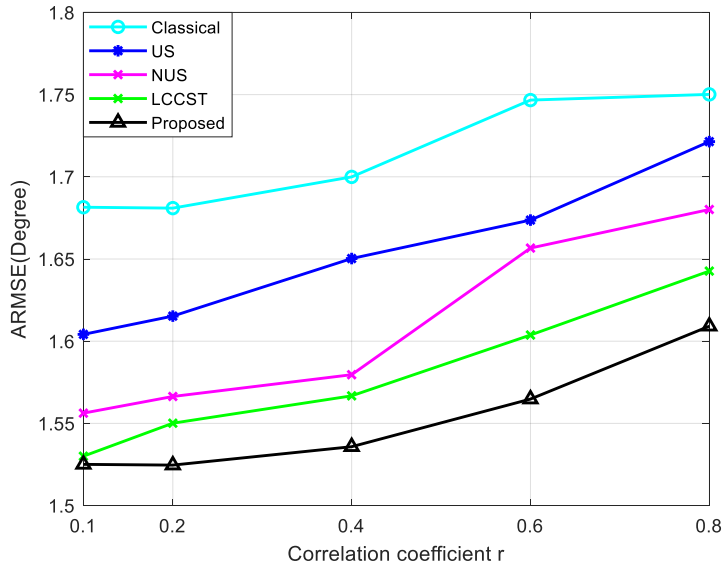

Fig. 10. Comparison of accuracy (ARMSE) between the VoST and existing sampling techniques, considering different correlation levels between incoming signals.

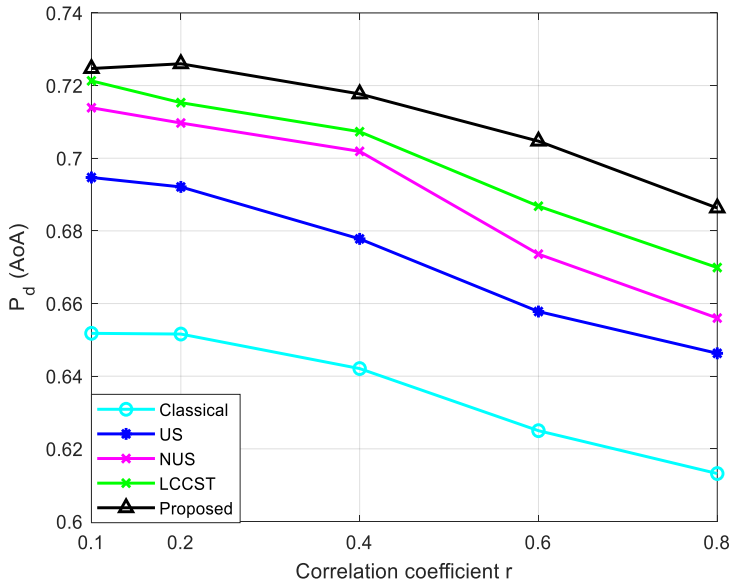

Fig. 11. Comparison of accuracy (P_d) between the VoST and existing sampling techniques, considering different correlation levels between incoming signals.

To compute the correlation level between arrived signals, we apply the well-known Pearson correlation coefficient [29] as follows:

$$r = \frac{\sum(x_i-\bar{x})(y_i-\bar{y})}{\sqrt{\sum(x_i-\bar{x})^2\sum(y_i-\bar{y})^2}} \quad (28)$$

where r is the Pearson correlation coefficient. x_i and y_i are the individual elements of signals x and y. $\bar{x}$ and $\bar{y}$ denote the mean values of signals x and y.

Based on the data shown in the figures, it is evident that the proposed technique reaches the highest accuracy relative to the compared algorithms when the incident signals are either weakly ($r = 0.1$) or strongly ($r = 0.8$) correlated. Therefore, this superiority of the proposed technique comes from the fact that the proposed sampling technique makes VoPM more robust against the correlated signals. It is also shown that the CT is least robust to these types of signals, with the UT, NUT, and LCCST following in that order.

6.4. Complexity Comparisons

As previously stated, the existing sampling techniques require $O(M^2L)$ mathematical operations to formulate the PM. Whereas, the suggested technique reduces this computational burden to $O(M^2(L-1)$. To exemplify this advantage, we take the antenna array having the above-mentioned specifications with varying the number of detected sources. Next, we calculate the computational burden of the proposed technique and compare it with that of existing methods in literature. The achieved result is illustrated in Fig. 12. The figure clearly confirms the theoretical analysis presented in Section 5. This feature of the proposed technique is due to using sparse matrices (i.e., ODCM) which make operations faster by working with smaller and more manageable datasets.

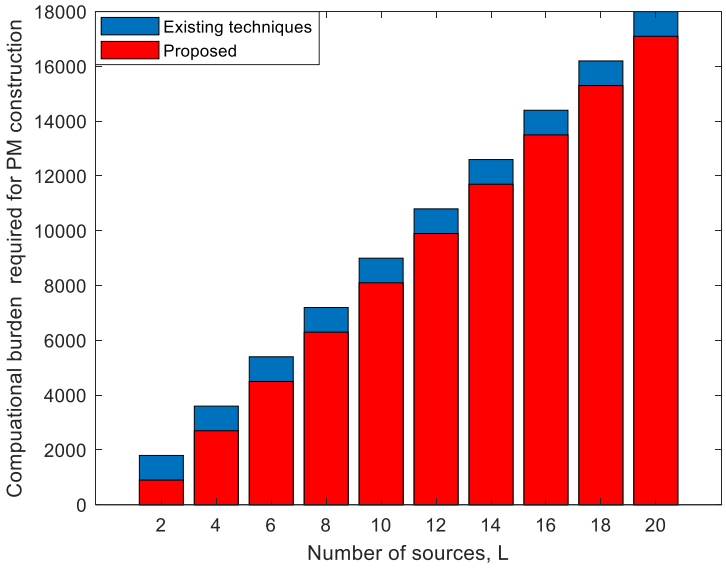

Fig. 12. Comparing the computational complexity of PM construction between the proposed and existing methods.

6.5. Execution Time Comparison

The mean execution time for columns selection and the PM construction based on different techniques are computed and compared in this section. The simulation parameters for this scenario are chosen as $M = 30, N = 100, L = 12$, $SNR = 0$ dB. The property of the machine used in this scenario is Intel CPU i7-1255U (1.7 GHz), 8GB Installed RAM.

The column selection process in CT is relatively simple, which makes it the fastest algorithm. This simplicity in the selection of columns, however, results in inadequate performance as illustrated in the previous section. The data listed in Table 6 shows that the

proposed algorithm is much faster than its counterparts (i.e., UT, NUT, and LCCST). This improvement stems from excluding the signal variances sit on the main diagonal of the CM (processing ODCM instead of CM). It is important to note that the execution time will be different from that presented here depending on the capability of the PC used for the computation and the simulation setting. The relative execution time, however, must be the same.

Table 6. Mean execution time comparison for different techniques.

Algorithm	CT	UT	NUT	LCCST	Proposed
Execution time [s]	1.1592	2.3521	2.5709	3.1047	1.3261

6.6. Overall Comparison between LCCST and VoST

To summarize the experimental outcomes and highlight the main distinctions between the recently developed LCCST [21] and the proposed VoST algorithm, an overall comparison is presented in Table 7. This table consolidates both qualitative and quantitative performance indicators, including computational complexity, estimation accuracy, robustness under correlated sources, and execution time. The results clearly demonstrate that VoST achieves superior accuracy and robustness while maintaining significantly lower computational complexity.

Table 7. Quantitative and qualitative comparison between LCCST and VoST.

Criterion	LCCST [21]	Proposed VoST	Improvement / Observation
Sampling principle	Includes main diagonal (signal variances) in correlation computation	Omits main diagonal and uses off-diagonal covariance only	More accurate correlation-level calculation
PM complexity	$O(M^2L)$	$O\left(M^2\,(L-1)\right)$	≈ 10–15 % reduction in total operations for moderate (L)
Mean execution time (s)	3.1047 s	1.3261 s	≈ 80 % faster
Average RMSE at SNR = 0 dB	≈ 0.725°	≈ 0.675°	≈ 8 % reduction in error
Probability of successful detection (P_d) SNR = 0 dB	≈ 0.681	≈ 0.7	≈ 3 % higher detection rate
Performance under correlated signals	Significant degradation	Maintains stable accuracy	More robust to correlation
Resolution (No. of detectable sources)	Fails to resolve all nine closely spaced sources	Successfully detects all the nine sources	Higher angular resolution
Memory usage	High, due to dense CM processing	Lower, due to sparse off-diagonal CM	More efficient implementation
Overall assessment	High accuracy but computationally intensive	Higher accuracy with reduced complexity and faster convergence	VoST provides superior trade-off between accuracy and efficiency

7. CONCLUSION

This work has presented the VoST as a significant enhancement for efficient AOA estimation. The proposed sampling technique selects the columns with the lowest dependency in the ODCM, ensuring that the PM is constructed using only unique and non-redundant information. By omitting the signal variance and focusing on the ODCM elements, the VoST effectively reduces computational load while improving estimation precision and detection capabilities. In contrast to the classical and the newly developed methods, the proposed algorithm accurately detected all AOAs and effectively resolved closely spaced sources with high resolution. Comparative analysis with existing techniques highlights the superior performance of VoST, particularly in terms low ARMSE, high probability of successful detections, high computational-efficiency, high robustness against signal correlation, and fast convergence. The proposed method thus addresses the key limitations of the previous sampling approaches, offering a promising solution for real-time AOA estimation in current and future wireless communication networks.

Declarations

Funding: No funding was received to assist with the preparation of this manuscript**.**

Conflicts of interest/Competing interests: The authors have no relevant financial or non-financial interests to disclose.

REFERENCES

[1] H. Krim, M. Viberg, "Two decades of array signal processing research: the parametric approach," *IEEE signal processing magazine,* vol. 13, no. 4, pp. 67-94, 1996, doi: 10.1109/79.526899.

[2] B. Karim, H. Ali, "Computationally efficient MUSIC based DOA estimation algorithm for FMCW radar," *Journal of Electronic Science and Technology,* vol. 21, no. 1, p. 100192, 2023, doi: 10.1016/j.jnlest.2023.100192.

[3] B. Karim, "Low-complexity AOA estimation for FMCW radar using projection-based subspace approximation," *Telecommunication Systems,* vol. 88, no. 3, p. 81, 2025, doi: 10.1007/s11235-025-01311-0.

[4] L. Wan, G. Han, L. Shu, S. Chan, T. Zhu, "The application of DOA estimation approach in patient tracking systems with high patient density," *IEEE Transactions on Industrial Informatics,* vol. 12, no. 6, pp. 2353-2364, 2016, doi: 10.1109/TII.2016.2569416.

[5] P. Li, X. Zhang, W. Zhang, "Direction of arrival estimation using two hydrophones: Frequency diversity technique for passive sonar," *Sensors,* vol. 19, no. 9, p. 2001, 2019, doi: 10.3390/s19092001.

[6] J. Arceo-Olague, D. Rosales, J. Luna-Rivera, A. Ángeles-Valencia, "Efficient adaptive algorithms for DOA estimation in wireless communications," *International Journal of Communications, Network and System Sciences,* vol. 3, no. 2, pp. 173-176, 2010, doi: 10.4236/ijcns.2010.32024.

[7] B. Karim, H. Ali, "A novel beamforming technique using mmWave antenna arrays for 5G wireless communication networks," *Digital Signal Processing,* vol. 134, p. 103917, 2023, doi: 10.1016/j.dsp.2023.103917.

[8] E. Larsson, O. Edfors, F. Tufvesson, T. Marzetta, "Massive MIMO for next generation wireless systems," *IEEE communications magazine,* vol. 52, no. 2, pp. 186-195, 2014, doi: 10.1109/MCOM.2014.6736761.

[9] J. Wang, B. Shi, F. Shu, Q. Zhang, D. Wu, Q. Jie, Z. Zhuang, S. Feng, Y. Zhang, "DOA estimation using massive receive MIMO: basic principle and key techniques," *arXiv preprint arXiv:2109.00154,* 2021, doi: 10.48550/arXiv.2109.00154.

[10] J. Capon, "High-resolution frequency-wavenumber spectrum analysis," *Proceedings of the IEEE,* vol. 57, no. 8, pp. 1408-1418, 1969, doi: 10.1109/PROC.1969.7278.

[11] R. Schmidt, "Multiple emitter location and signal parameter estimation," *IEEE transactions on antennas and propagation,* vol. 34, no. 3, pp. 276-280, 1986, doi: 10.1109/TAP.1986.1143830.

[12] S. Reddi, "Multiple source location-a digital approach," *IEEE Transactions on Aerospace and Electronic Systems,* no. 1, pp. 95-105, 1979, doi: 10.1109/TAES.1979.308800.

[13] R. Roy, T. Kailath, "ESPRIT-estimation of signal parameters via rotational invariance techniques," *IEEE Transactions on acoustics, speech, and signal processing,* vol. 37, no. 7, pp. 984-995, 1989, doi: 10.1109/29.32276.

[14] J. Munier, G. Delisle, "Spatial analysis using new properties of the cross-spectral matrix," *IEEE Transactions on Signal Processing,* vol. 39, no. 3, pp. 746-749, 1991, doi: 10.1109/78.80863.

[15] S. Marcos, A. Marsal, M. Benidir, "The propagator method for source bearing estimation," *Signal processing,* vol. 42, no. 2, pp. 121-138, 1995, doi: 10.1016/0165-1684(94)00122-G.

[16] Y. Wang, A. Singh, "Provably correct algorithms for matrix column subset selection with selectively sampled data," *Journal of Machine Learning Research,* vol. 18, no. 156, pp. 1-42, 2018, doi: 10.48550/arXiv.1505.04343.

[17] R. Schreiber, "Implementation of adaptive array algorithms," *IEEE transactions on acoustics, speech, and signal processing,* vol. 34, no. 5, pp. 1038-1045, 1986, doi: 10.1109/TASSP.1986.1164943.

[18] P. Comon, G. Golub, "Tracking a few extreme singular values and vectors in signal processing," *Proceedings of the IEEE,* vol. 78, no. 8, pp. 1327-1343, 1990, doi: 10.1109/5.58320.

[19] M. Al-Sadoon, M. Ree, R. Abd-Alhameed, P. Excell, "Uniform sampling methodology to construct projection matrices for Angle-of-Arrival estimation applications," *Electronics,* vol. 8, no. 12, p. 1386, 2019, doi: 10.3390/electronics8121386.

[20] M. Al-Sadoon, M. Mosleh, N. Ali, H. Migdadi, R. Abd-Alhameed, P. Excell, "Construction of projection matrices based on non-uniform sampling distribution for AoA estimation," *IEEE Access,* vol. 8, pp. 98369-98382, 2020, doi: 10.1109/ACCESS.2020.2993908.

[21] B. Karim, H. Ali, M. Al-Sadoon, "A novel sampling methodology exploiting the least correlated-columns for angle of arrival estimation," *Physical Communication,* vol. 55, p. 101878, 2022, doi: 10.1016/j.phycom.2022.101878.

[22] J. Pan, M. Sun, Y. Wang, X. Zhang, "An enhanced spatial smoothing technique with ESPRIT algorithm for direction of arrival estimation in coherent scenarios," *IEEE Transactions on Signal Processing,* vol. 68, pp. 3635-3643, 2020, doi: 10.1109/TSP.2020.2994514.

[23] B. Karim, H. Ali, "A new improved algorithm for low complexity wideband angle of arrival estimation," *International Journal of Electrical and Electronic Engineering & Telecommunications,* vol. 11, no. 6, pp. 398-409, 2022, doi: 10.18178/ijeetc.11.6.398-409.

[24] W. Deng, J. Li, Y. Tang, X. Zhang, "Low-complexity joint angle of arrival and time of arrival estimation of multipath signal in uwb system," *Sensors,* vol. 23, no. 14, p. 6363, 2023, doi: 10.3390/s23146363.

[25] J. Shen, F. Gini, M. Greco, T. Zhou, "Off-grid DOA estimation using improved root sparse Bayesian learning for non-uniform linear arrays," *EURASIP Journal on Advances in Signal Processing,* vol. 2023, no. 1, p. 34, 2023, doi: 10.1186/s13634-023-00991-7.

[26] M. Ahmad, X. Zhang, X. Lai, F. Ali, X. Shi, "Low-complexity 2D-DOD and 2D-DOA estimation in bistatic MIMO radar systems: A reduced-dimension MUSIC algorithm approach," *Sensors,* vol. 24, no. 9, p. 2801, 2024, doi: 10.3390/s24092801.

[27] S. El-Khamy, A. El-Shazly, A. Eltrass, "A compressive sensing based computationally efficient high-resolution DOA estimation of wideband signals using generalized coprime arrays," *Wireless Personal Communications,* vol. 134, no. 3, pp. 1571-1597, 2024, doi: 10.1007/s11277-024-10969-9.

[28] Y. Yang, J. Wang, Z. Wang, "Coherent DOA estimation based on low-rank matrix recovery with coprime arrays in nonuniform noise," *EURASIP Journal on Advances in Signal Processing,* vol. 2025, no. 1, p. 3, 2025, doi: 10.1186/s13634-025-01206-x.

[29] J. Rodgers, W. Nicewander, "Thirteen ways to look at the correlation coefficient," *The American Statistician,* vol. 42, no. 1, pp. 59-66, 1988, doi: 10.1080/00031305.1988.10475524.